Numerical Simulation of Exterior Condensations on Façades: The Undercooling Phenomenon

J.M.P.Q. Delgado, PhD **V.P. de Freitas, PhD**
N.M.M. Ramos, PhD **E. Barreira**

ABSTRACT

This manuscript presents a brief state-of-the-art on the development and application of hygrothermal analysis methods to simulate the coupled transport processes of heat and moisture for one or multidimensional cases.

This work intends to apply existing numerical models of exterior boundary conditions on the simulation of exterior condensation on façades (undercooling phenomenon) finished with external thermal insulation composite systems (ETICS). The results of three hygrothermal models were compared, regarding the temperature on the exterior surface of a west façade. The climatic conditions from the city of Porto, Portugal were used. We analyzed in detail how the simulation of the undercooling phenomenon is influenced by the numerical treatment of the radiative balance on the exterior surface.

The numerical results show that these programs are useful tools in assessing the exterior condensation on façades and the importance of radiative balance on the exterior surface temperature. However, some differences were observed in the calculated values due to different parameters included in the radiative balance of the models.

INTRODUCTION

The problem of moisture damage in buildings has attracted interest from the early days of the last century, but it was only with the development of the modeling of hygrothermal performance that the general topic of moisture transport in buildings became the subject of more systematic study. Moisture behavior may induce damage in buildings, and this increasingly demands for calculation methods in building engineering to assess the moisture behavior of building components. Over the last five decades, hundreds of building energy software tools have been developed or enhanced to be used. A list of such tools can be obtained in http://www.eere.energy.gov/buildings/tools_directory. This directory provides information for more than 345 building software tools for evaluating energy efficiency, renewable energy and sustainability in buildings.

In the area of building physics the hygrothermal models are widely used to simulate the coupled transport processes of heat and moisture for one or multidimensional cases. The models may take into account a single component of the building envelope in detail or a multizonal building. In literature, there are many computer-based tools for the prediction of the hygrothermal performance of buildings. These models vary significantly concerning their mathematical sophistication and, as shown by Straube and Burnett (2001), this sophistication depends on the degree that takes into consideration the following parameters: moisture transfer dimension; type of flow (steady-state, quasi-static, or dynamic); quality and availability of information and stochastic nature of each data (material properties, weather, construction quality, etc.).

The HAM models (heat, air, and moisture) combine the flow equations with the mass and energy balances. Transient, one-dimensional models for combined heat, air, and moisture transport in building components have been reasonably well established for about two decades now. In 1996 the final report of Volume 1—Modelling, of the Annex 24 of the International Energy Agency (IEA), edited by H. Hens, showed that 37 programs had been developed by researchers of 12 countries,

J.M.P.Q Delgado *is an assistant researcher,* ***V.P. de Freitas*** *is a full professor,* ***N.M.M. Ramos*** *is an assistant professor, and* ***E. Barreira*** *is a lecturer in the Civil Engineering Department (DEC) at the Faculdade de Engenharia da Universidade do Porto, Porto, Portugal.*

26 of which were non-steady state models. In the last ten years, many programs indicated in this work have developed new versions and improved the conditions of analysis and results reliability. More recently (in 2003), a review of hygrothermal models for building envelope retrofit analysis made by Canada Mortgage and Housing Corporation (CMHC) has identified 45 hygrothermal modeling tools (CMHC 2003), and in the last four years, 12 new hygrothermal models were developed, more of them during Annex 41 (see Table 1).

However, most of the 57 hygrothermal models available in literature are not readily available to the public outside of the organization in which they were developed. In fact, only 14 hygrothermal modeling tools are available to the public in general. The following 9 commercial programs: 1D-HAM, Sim2000, DELPHIN, GLASTA, hygIRC-1D, IDA-ICE, MATCH, MOISTURE-EXPERT and WUFI; and the 5 free-ware programs: EMPTIED, HAMLab, HAM-Tools, MOIST and UMIDUS.

The programs available for the public in general were analyzed in detail (see Table 1), namely the input of material properties and the boundary conditions (inside and outside). An elaborate classification of numerical tools used to simulate the transport of Heat-Air-Moisture in buildings was presented

Table 1. Information of the 14 Hygrothermal Models Available to the Public in General

Name	Type	Material Properties														Boundary Conditions (outside)										B.C. (inside)			
		1	2	3	4	5	6	7	8	9	10	11	12	13	14	A	B	C	D	E	F	G	H	I	J	I	II	III	IV
1D-HAM	1D-HAM	X		X	X	X	X							X		X	X	X	X				X			X	X		
BSim2000	1D-HM	X	X	X	X	X	X						X		X	X	X	X	X	X	X		X	X		X	X	X	
DELPHIN 5	1/2D-HAMPS	X	X	X	X	X		X	X	X		X		X		X	X	X	X	X	X	X	X			X	X	X	
EMPTIED	1D-HAM	X		X	X		X		X					X		X	X	X								X	X	X	
GLASTA	1D-HM	X		X	X		X	X								X	X		X				X			X			
hygIRC-1D	1D-HAM	X		X	X	X	X		X	X				X		X	X		X	X	X	X		X	X	X	X		X
HAMLab	1D-HAM	X		X	X			X			X		X			X	X			X	X		X	X		X	X		
HAM-Tools	1D-HAM	X	X	X	X	X	X		X			X		X		X	X	X	X	X	X	X	X	X		X	X	X	
IDA-ICE(*)	1D-HAM	X		X	X	X	X						X	X		X	X	X	X	X	X		X			X	X		
MATCH	1D-HAM	X	X	X	X	X	X		X			X	X		X	X	X		X	X		X	X	X		X	X		
MOIST	1D-HM	X		X	X	X	X		X	X				X		X	X		X	X	X			X		X	X		
MOIST-EXP.	1/2D-HAM	X	X	X	X	X	X		X	X		X	X	X		X	X	X	X	X	X	X	X	X	X	X	X	X	X
UMIDUS	1D-HM	X	X	X	X	X		X								X	X		X	X	X					X	X		
WUFI (**)	1/2D-HM	X	X	X	X	X	X			X	X	X	X			X	X		X	X	X	X	X	X		X	X		

(*) IDA-ICE version with HAMWall
(**) WUFI family: WUFI-Plus, WUFI-2D, WUFI-Pro and WUFI-ORNL/IBP. A free research and education version of WUFI-ORNL/IBP for USA and Canada is available.

List of Symbols

1–Bulk density
2–Porosity
3–Specific heat capacity
4–Thermal conductivity
5–Sorption isotherm
6–Vapour permeability
7–Vapour diffusivity
8–Suction pressure
9–Liquid diffusivity
10–Diff resistance factor
11–Water conductivity
12–Specific moisture capacity
13–Air permeability
14–Hysteresis in sorption isotherm
A–Temperature
B–RH / Humidity ratio / Dew point / Vapour pressure/concentration
C – Air pressure
D – Solar radiation
E – Wind velocity
F– Wind direction
G–Precipitation
H–Long-wave exchange
I–Cloud index
J–Water leakage
I–Temperature
II–RH / Humidity ratio / Dew point / Vapour pressure/ concentration
III–Air pressure
IV–Interior stack effect (T and RH)

in a ASTM publication (Trechsel 2001). A critical element in the design of wall systems is related to the exterior and interior hygrothermal environmental loads. The most important exterior environmental loads (influence directly the transport of heat and moisture) are: (1) ambient temperature; (2) ambient relative humidity; (3) solar diffuse; (4) solar direct; (5) cloud index; (6) wind velocity; (7) wind orientation; and (8) horizontal rain.

Finally, as the purpose of most hygrothermal models is usually to provide sufficient and appropriate information needed for decision-making, we suggested three items that should be used when modeling a single component of the building envelope or a multizonal building: (1) the software must be available in the public domain (freeware or commercially); (2) suitability of the software for the single component or a multizonal building analyze under consideration; and (3) the software must be "user friendly".

One important characteristic of HAM models is the ability to simulate the radiative balance in the exterior surface. In fact, most models use a simplified method to assess surface temperature on the exterior layer that only considers explicitly the effect of solar radiation. The effect of the long-wave radiation exchange is modelled as a constant parameter, independent of the surface itself, and is included in the heat transfer coefficient value.

Solar radiation, considered as a source of heat that increases the surface temperature during the day, depends on short-wave radiation absorptivity, α_s, and on the solar radiation normal to component surface, I_s (Hagentoft 2001).

$$q_s = \alpha_s \times I_s \tag{1}$$

The heat flux, q_{cl}, between the surface and the exterior air is given by their temperature differences, T_s and T_a. The heat transfer coefficient, h, consists in two parts, one dealing with convection, h_c, and the other with long-wave radiation, h_r.

$$q_{cr} = h \times (T_a - T_s) \tag{2}$$

$$h = h_c + h_r \tag{3}$$

The radiative heat transfer coefficient, h_r, specifies the long-wave radiation exchange between the building surface and other terrestrial surfaces (sky included), that is governed by the Stefan-Boltzmann Law (σ is the Stefan-Boltzmann constant). As all surrounding surfaces of the building have similar temperatures, the heat flux, q_r, dependent on the fourth power of the temperature, can be linearized in good approximation. Since normally the temperatures of the terrestrial surfaces are not known, they are assumed to be identical to the air temperature. Furthermore, it is also assumed that all objects have similar emissivities, ε, as long as they are non-metallic, which is usually the case in the context of building physics. Three of the four powers of the temperature are lumped together with the radiative heat transfer coefficient, and a simple linear relationship analogous to the convective heat transfer is obtained (Hagentoft 2001).

$$q_r = \varepsilon_t \times \sigma \times T_a^4 - \varepsilon_s \times \sigma \times T_s^4 \approx h_r \times \langle T_a - T_s \rangle \tag{4}$$

$$h_r = 4 \times \varepsilon \times \sigma \times T_0^3 \tag{5}$$

where T_0 is an average temperature depending on the surface, the surrounding surfaces and the sky.

Although these temperatures change in time, in most formulations they are assumed as constant. Providing that outside surfaces have similar emissivity, a constant value for the radiative heat transfer coefficient may be adopted. This simplification is quite appropriate for most hygrothermal simulations, however to assess the undercooling phenomenon in walls covered with external thermal insulation composite systems (ETICS), more accuracy in the exterior layer is needed. The low thermal capacity of the external rendering and its thermal decoupling emphasizes the influence of boundary conditions, mainly temperature and radiation.

It is known that undercooling phenomenon, which occurs mostly during the night, is caused by long-wave radiation exchange between the exterior surface and its surroundings. The radiant balance of a building façade is affected by the building's radiation, the sky's radiation, and terrestrial surface's radiation (Barreira et al. 2009). A building, being a grey body, emits long-wave radiation that can be calculated using the Stefan-Boltzmann Law. On the other hand, the façade absorbs part of the long-wave radiation emitted by surrounding surfaces and by the sky. Terrestrial radiation is the sum of long-wave radiation emitted by the terrestrial surfaces (ground, other building façades, obstacles, etc.) that also behave as grey bodies and whose temperature is similar to the building's temperature. Therefore, terrestrial surfaces and the building emit long-wave radiation at identical intensities.

Atmosphere may behave in two distinct manners. If the sky is cloudy, the atmosphere behaves like a grey body whose temperature is identical to the building's, and emits radiation in a continuous spectrum at intensity similar to that of terrestrial surfaces. If the sky is clear, the atmosphere stops emitting continuously for all wavelengths and the atmosphere's emitted radiation decreases considerably. The radiation emitted by the surface is, therefore, greater than the one that reaches the surface, causing a loss of radiation.

This negative balance that is not compensated by solar radiation during the night causes the building's surface temperature to decrease, which is maintained until heat transport by convection and by conduction compensate for the loss by radiation. Condensation takes place whenever the surface temperature is lower than the dew point temperature.

For this reason, the influence on the exterior surface temperature of the numerical treatment of the radiative balance will be analyzed in detail in the following paragraphs.

CASE STUDIES

The Overview of Used Programs. Hygrothermal modelling offers a powerful tool for predicting heat and moisture transport through multi-layer building assemblies. In this

work, three hygrothermal models were used to compare the results of a case study under natural conditions. These simulations used generate climatic variables and actual material properties to determine temperature dynamics.

Model 1 was validated using data derived from outdoor and laboratory tests, and allows realistic calculation of the transient hygrothermal behavior of multi-layer building components exposed to natural climate conditions (Kuenzel and Kiessl 1997). The governing equations for moisture and energy transfer are, respectively,

$$\frac{\partial w}{\partial \varphi}\frac{\partial \varphi}{\partial t} = \nabla(D\varphi\nabla\varphi + \delta_p\nabla(\varphi p_{sat})) \tag{6}$$

$$\frac{\partial H}{\partial T}\frac{\partial T}{\partial t} = \nabla(\lambda\nabla T) + h_v\nabla(\delta_p\nabla(\varphi p_{sat})) \tag{7}$$

where $\partial H/\partial T$ is the heat storage capacity of the moist building material, $\partial w/\partial \varphi$ is the moisture storage capacity, w is the moisture content, λ is the thermal conductivity, D_φ is the liquid conduction coefficient, δ_p is the water vapor permeability, h_v is the evaporation enthalpy of the water, p_{sat} is the water vapor saturation pressure, T is the temperature, and φ is the relative humidity.

Model 2 is a one-dimensional simulation tool for modelling heat, air, and moisture movement in exterior walls. More details may be found in Karagiozis (1993, 1997), Karagiozis et al. (1996) and Djebbar et al. (2002a,b). The governing equations for moisture, heat, air mass, and momentum balance are, respectively,

$$\frac{\partial w}{\partial t} + \nabla(u\rho_v + K\rho_w g) = \nabla(D_w\nabla w + \delta_p\nabla p_{sat}) + m_s \tag{8}$$

$$\begin{aligned} &c_p\rho\frac{\partial T}{\partial t} + \nabla(u\rho_a c_{pa}T) \\ &= \nabla(\lambda\nabla T) + L_v(\nabla(\delta_p\nabla p_{sat})) - L_{ice}\left(w\frac{\partial f_l}{\partial t}\right) + Q_s \end{aligned} \tag{9}$$

$$\nabla(\rho_a u) = 0 \tag{10}$$

$$-\nabla\left(p_a\frac{k_a}{\eta}\nabla P\right) = 0 \quad \text{with} \quad u = -\frac{k_a}{\eta}\nabla P \tag{11}$$

where u is the air velocity, ρ_v is the water-vapor density, K is the liquid-water permeability, ρ_w is the density of water, g is the acceleration due to gravity, D_w is the moisture diffusivity, m_s is the moisture source, c_p is the effective heat capacity, ρ is the dry density of the material, ρ_a is the density of air, c_{pa} is the specific capacity of air, L_v is the latent heat of evaporation/condensation, L_{ice} is the latent heat of freezing/melting, f_l is the fraction of water frozen, Q_s is the heat source, k_a is the air permeability, and η is the dynamic viscosity.

Finally, Model 3 is a building simulation software, for one-dimensional heat, air, and moisture transfer (Kalagasidis 2004). This program uses the graphical programming language Simulink®. The software is an open source, new modules can be easily added by users, and they are free of charge and can be downloaded from the internet. The governing equations for moisture and energy transfer are

$$\frac{\partial w}{\partial t} = -\frac{\partial}{\partial x}\left(K\frac{\partial s}{\partial x} - \delta_p\frac{\partial p}{\partial x} + g_a u\right) \tag{12}$$

$$\rho c_p\frac{\partial T}{\partial t} = -\frac{\partial}{\partial x}\left(-\lambda\frac{\partial T}{\partial x} + g_a c_{pa}T + g_v L_v\right) \tag{13}$$

where s is the suction pressure, g_a is the air flux density and g_v is the water vapor flux density.

Regarding the treatment of the radiation effect on the exterior surface, all three models use an explicit balance of the long-wave radiation, defining the surface emission, I_e, and the radiation arriving to it, I_l. They are combined with the short-wave radiation components into a collective heat source at the surface which may have positive or negative value, depending on the overall radiation balance: a positive value leads to heating up the component and a negative value leads to cooling it. With this methodology, the exterior heat transfer coefficient only contains the convective part.

$$q = \alpha_s \times I_s + \varepsilon_{l,\,surf} \times I_l - I_e \tag{14}$$

In Equation 14, the two first items give the total amount of radiation (short and long) arriving to the surface, as according to Kirchoff Law the emissivity of a surface, $\varepsilon_{l,surf}$, is equal to its long-wave absorptivity. The last item is the radiation emitted by the building surface.

The total solar radiation, I_s, is described as a function of the direct solar radiation normal to component surface, $I_{s,dir}$, of the diffuse solar radiation, $I_{s,dif}$, affected by the atmospheric field of view, g_{atm}, and of the solar radiation reflected by the ground, $I_{s,ref}$, affected by the field of view of the ground, g_{ter}.

$$I_s = I_{s,\,dir} + g_{atm} \times I_{s,\,dif} + g_{ter} \times I_{s,\,ref} \tag{15}$$

The total long-wave radiation arriving to the surface, I_l, depends on the downward atmospheric radiation, $I_{l,atm}$, affected by the atmospheric field of view, g_{atm}.

$$I_l = g_{atm} \times I_{l,\,atm} \tag{16}$$

The sky radiation is ruled by the Plank Law, considering the concept of effective sky temperature, which can be defined as the temperature of a blackbody that emits the same amount of radiation as the sky (Martin and Berdahl 1984). The effective sky temperature depends on several atmospheric conditions, which is rarely available. For that reason, it is assumed that the sky behaves like a grey body, ruled by Stefan-Boltzmann Law, considering the sky emissivity and the air temperature near the ground (Finkenstein and Haupl 2007).

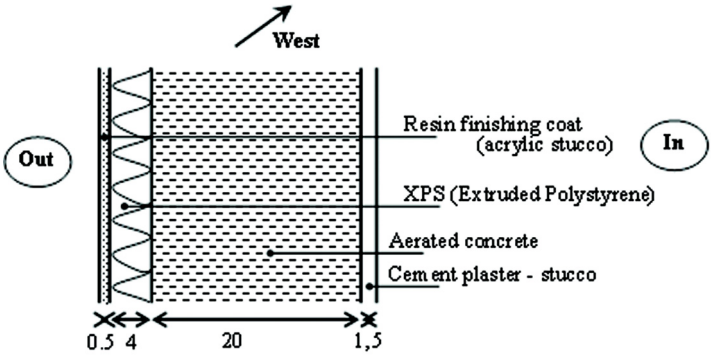

Figure 1 *Wall construction details (dimensions in cm).*

Table 2. Material Properties of Wall Components used in the Hygrothermal Models

Wall Components	L (mm)	ρ (kg/m^3)	ε (m^3/m^3)	λ (W/mK)	c_p (J/kgK)	μ (—)
Resin finishing coat (acrylic stucco)	5	1800	0.12	0.70	840	1000
EPS (Expanded polystyrene)	40	15	0.95	0.04	1500	30
Concrete C12/C15	200	2200	0.18	1.6	850	92
Cement plaster—stucco	15	1985	0.30	1.20	840	25

The downward atmospheric radiation in a specific location may be obtained through measurement, using pyrgeometers, or by empirical models (detailed methods are not commonly used because they require the knowledge of atmospheric conditions). According to Finkenstein and Haupl (2007), those empirical models provide satisfactory results for clear sky but the approaches for cloudy sky still point to very different results. The long-wave radiation emitted by the surface, I_e, depends on the surface emissivity, $\varepsilon_{l,surf}$, and temperature, T_{surf}, as it is ruled by the Stefan-Boltzmann Law.

$$I_e = \varepsilon_{l,\,surf} \times \sigma \times T_{surf}^4 \tag{17}$$

From the above equations, the direct solar radiation normal to component surface, $I_{s,dir}$, is automatically calculated by each model from the direct solar radiation in an horizontal surface, included in the climatic data, using information about the sun position. The diffuse solar radiation, $I_{s,dif}$ is obtained directly from the climatic data. The solar radiation reflected, $I_{s,ref}$, is calculated using solar radiation data (direct in an horizontal surface and diffuse) and the short wave radiation reflectivity of the ground.

The differences between the three models, regarding the heat exchange by radiation in the exterior surface, are related with the way the long-wave radiation emitted by the sky is obtained and the effect of the ground in the balance.

Model 1 allows two different approaches to obtain the atmospheric long-wave radiation, $I_{l,atm}$, necessary for the calculation: it may be read directly from the climatic file, if it has this information available, or it may be calculated using the cloud index data. This model also considers the emission and reflection of long-wave radiation by the ground, adding two extra items to Equation 16: the long-wave radiation emitted by the ground, calculated by the Stefan-Boltzmann Law assuming that the ground has the same temperature as the air and inputting the ground long-wave emissivity, and the atmospheric long-wave radiation reflected by the ground, calculated using the atmospheric long-wave radiation, $I_{l,atm}$, and the long-wave radiation reflectivity of the ground.

Model 2 calculates the atmospheric long-wave radiation, $I_{l,atm}$, necessary for the simulation, using the cloud index information available in the climatic file. The effect of the ground (emission and reflection of long-wave radiation) is not taken into account.

Model 3 reads the atmospheric long-wave radiation, $I_{l,atm}$, necessary for the calculation directly from the climatic file. The effect of the ground (emission and reflection of long-wave radiation) is not included in the mathematical treatment.

Wall Construction Details. Figure 1is a schematic of the façade analyzed numerically and Table 2 presents the material properties used in this application. The construction type chosen for comparison of the three hygrothermal models was a wall covered with ETICS, exposed to solar radiation.

The exterior and interior *Sd* value used was zero (no coating) and the interior heat transfer coefficient was constant and equal to 8 W/m^{2}K. The exterior heat transfer coefficient only

contained the convective part and was considered independent from the wind (constant value of 17 W/m^{2}K).

Climate. All the calculations were done with climate data for Porto, Portugal provided by a software tool (METEOTEST 2008). This program calculates hourly values of all parameters using a stochastic model and the resulting weather data files are produced in a variety of formats. The weather data inputted to the models was temperature (°C), relative humidity (–), wind direction (°), wind speed (m/s), global solar radiation in a horizontal surface (W/m²) and diffuse solar radiation in a horizontal surface (W/m²). Model 1 also required information about air pressure (hPa), downward atmospheric radiation in a horizontal surface (W/m²) and cloud index (two climatic file were created, one with downward atmospheric radiation and other with cloud index). Model 2 also included information about the cloud index variation and Model 3 also demanded data about the air pressure (hPa) and the downward atmospheric radiation in a horizontal surface (W/m²). In the climatic files, rain was inputted equal to zero. The conditions of indoor air were constants, with RH = 60% and T = 20ºC (comfort values). The short-wave radiation absorptivity and the long-wave radiation emissivity considered were 0.4 (stucco-normal bright) and 0.9, respectively, and the initial conditions within the element were RH = 70% and T = 15º C. The ground short-wave reflectivity was 0.2, and for Model 1 the ground long-wave emissivity was 0.9 and the ground long-wave reflectivity was 0.1.

Surface condensation. The condensation on the surface was assessed by comparing the surface temperature with the dew point temperature of outdoor air. Whenever the surface temperature drops below the dew point temperature condensations occur. The risk of condensation was evaluated by the accumulated value of the positive differences between the dew point temperature of outdoor air and the surface temperature during a certain period of time.

RESULTS AND DISCUSSION

In this case study, simulations were done with three hygrothermal models to analyze the influence of the numerical treatment of the radiative balance in the exterior surface temperature of the wall in Figure 1. All input parameters, including material properties, climatic data, and initial conditions, were made to vary as little as possible between the models in order to ensure a fair comparison.

Model 1 requires as material properties bulk density (kg/m^3), porosity (m^3/m^3), heat capacity (J/kgK), water content (kg/m^3), liquid transport coefficient (suction and redistribution) (m^2/s), heat conductivity (W/mK), and diffusion resistance factor.

Model 2 requires similar material properties as Model 1 but uses different units. The material properties required for simulation are: air permeability (kg/mPas), thermal conductivity (W/mK), dry density (kg/m^3), dry heat capacity (J/kgK), sorption curve moisture content (kg/kg), suction pressure (Pa), water vapor permeability (kg/mPas), liquid moisture diffusivity (m^2/s), and water content (kg/kg). The liquid moisture diffusivity was assumed the same as the liquid transport coefficient by suction used in Model 1. The water content was converted from kg/m^3 to kg/kg simply by dividing by the density of the material, and to m^3/m^3 by dividing by the density of the material and multiplying by the density of water (1000 kg/m^3). The water vapor permeability and the suction pressure, s, were calculated using the water vapor diffusion resistance factor and the Kelvin equation (Galbraith et al., 1997), respectively.

The properties required by Model 3 are the density of the dry material (kg/m^3), open porosity (–), specific heat capacity of the dry material (J/kgK), thermal conductivity (W/mK), sorption isotherm, moisture capacity, water vapor permeability (kg/msPa), and liquid water conductivity (s).

Most of these properties were taken directly from the Model 1 database and adapted to be used in the other hygrothermal models.

Figures 2a to 2c show the minimum, maximum, and average surface temperature obtained for each hygrothermal model. It is possible to observe similar temperatures on a surface obtained using all the models. The existing differences in the maximum and average may be related with the calculations of the solar radiation normal to the surface that influences mostly the surface temperature during the day, but also after the sunset and at dawn. The differences in the minimum temperature can also be related with the formulation used to calculate the radiation emitted by the sky (Models 1a and 3 use downward atmospheric radiation in a horizontal surface calculated by meteorological software and Models 1b and 2 calculate themselves the radiation using cloud index information). Differences in the governing equations and the conversion of the material properties may also have some effects on surface temperatures.

Figure 3 shows the variation in time of the calculated surface temperatures during a winter day (January 23) and Figure 4 shows the accumulated degrees of condensation (or the sum of the positive differences between dew point temperature and the surface temperature) for the same day. It is possible to see that surface temperature drops below dew point temperature during the early morning hours for all models, due to the low thermal capacity of the system that allows the dissipation of the heat stored during the day in a few hours after sunset. Condensation occurs during this period of time.

There is, however, small differences between the models that induce the results presented in Figure 4. Comparing Models 1a and 1b, of which the only difference is the long-wave radiation used (in Model 1a the radiation used was calculated by meteorological software and in Model 1b was calculated by the equations included in the model using cloud index information), it shows that the values inputted for the long-wave radiation influence considerably the surface temperature and consequently the surface condensation. Figure 5 shows that the model used to calculate the atmospheric radiation induces significant differences in the obtained values. This is

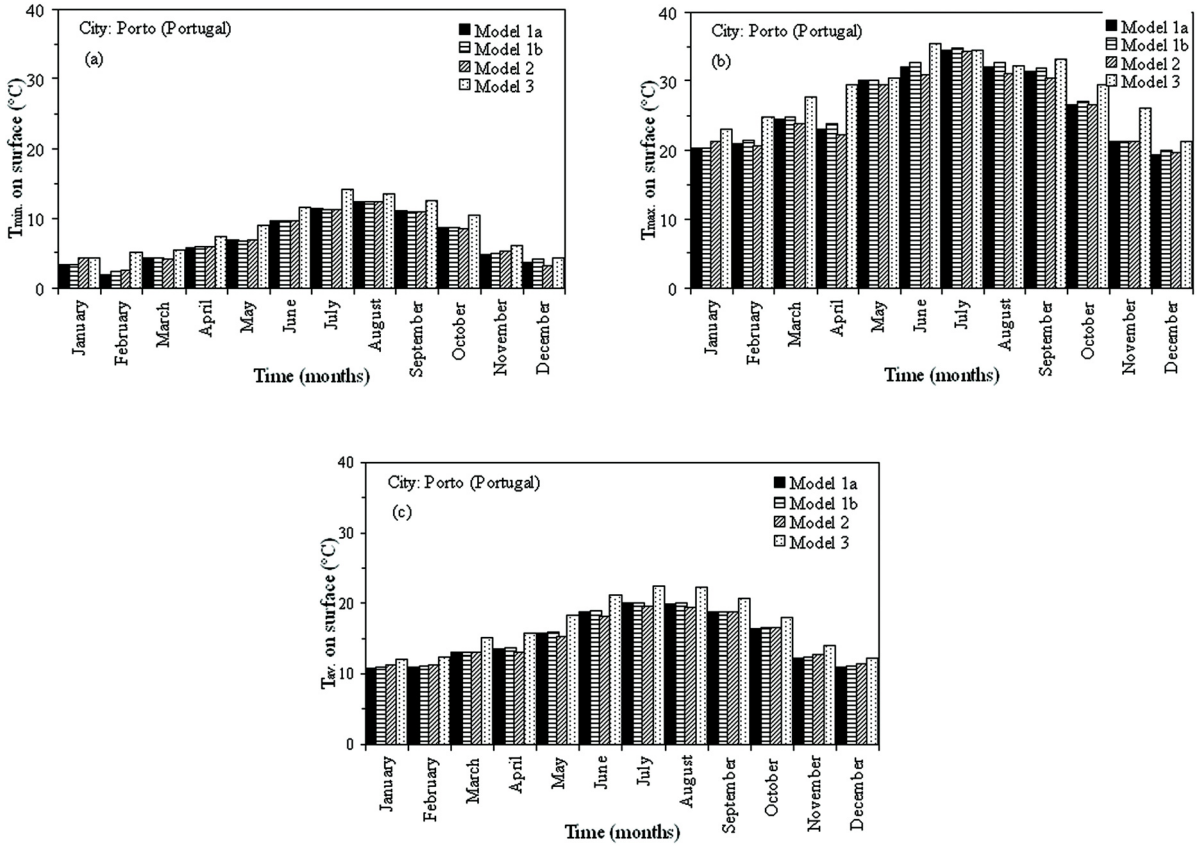

Figure 2 *Comparison of the surface temperature obtained with each hygrothermal model: (a) minimum temperature; (b) maximum temperature, and (c) average temperature.*

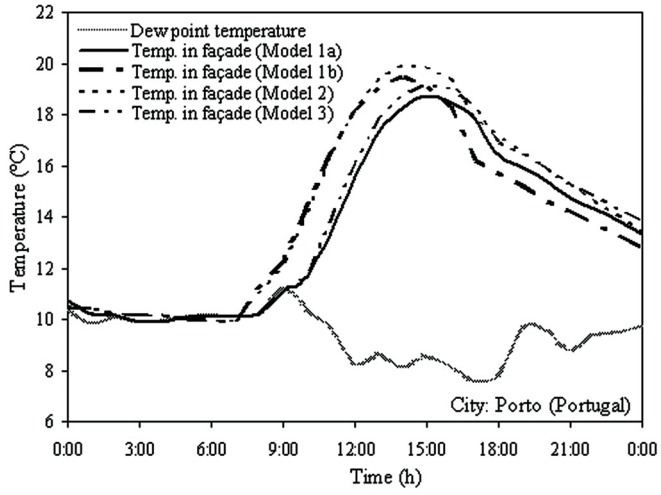

Figure 3 *Surface temperature obtained by each hygrothermal model for Porto (January 23).*

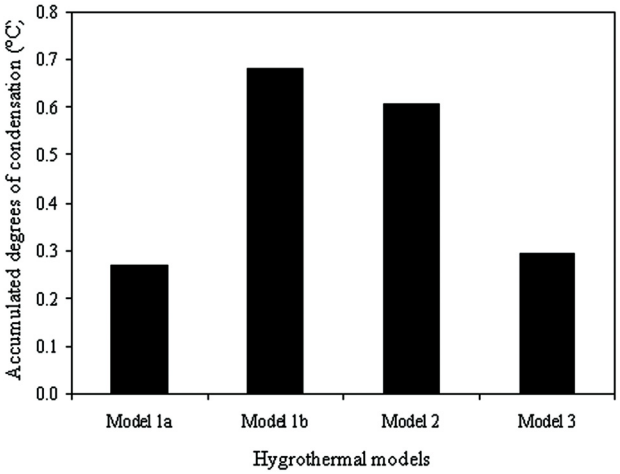

Figure 4 *Sum of positive differences between T_{dp} and T_{surf} for Porto (January 23).*

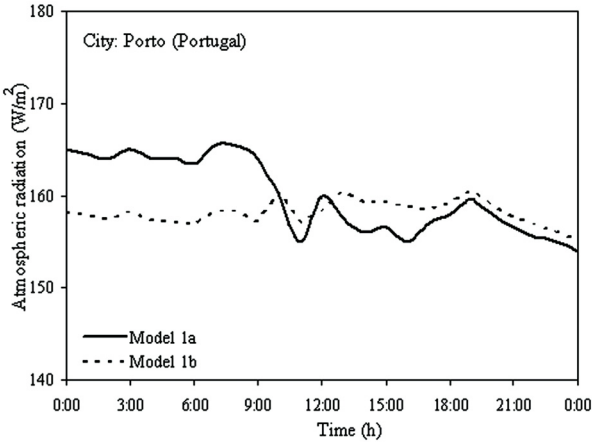

Figure 5 *Atmospheric radiation in a vertical plane in Porto (January 23).*

related with the difficulty in modeling atmospheric radiation with a cloudy sky, referred to previously in this paper. As radiation used in Model 1a is higher than the one used in Model 1b, surface temperatures are also higher and condensation is reduced.

Models 1b and 2 present very similar variation of the surface temperature, especially during the night. This points to the similarity of the models, not only in terms of governing equations but also in terms of boundary conditions. The effect of the ground included in Model 1a may not have much influence in the phenomenon or it may compensate some differences existing between the two models. The similar values obtained for the surface temperature are also shown in Figure 4, where the condensation values are also similar. Models 1a and 3 both use the atmospheric radiation calculated by the meteorological software and their results are quite similar. The considerations made previously for Models 1b and 2 can also be applied to this case.

Figure 6 displays monthly accumulated degrees of condensation. The results show that the most pronounced condensations occur during the late summer, fall, and winter months. This is related to the climatic conditions in Porto, a coastal town, namely its high relative humidity and mild temperatures year-round (Figures 7 and 8). However, it should be remarked, once more, that the effect of long-wave radiation is quite clear, as Models 1a and 3 have similar results and Models 1b and 2 also have similar results, but these two groups don't match. In fact, the last two models (Models 1b and 2)

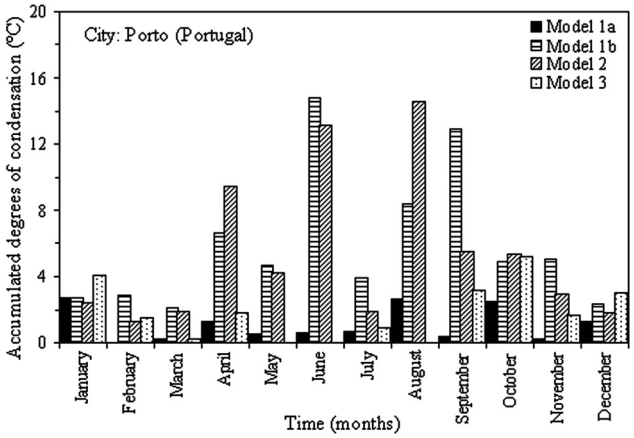

Figure 6 *Sum of positive differences between Tdp and Tsurf for Porto.*

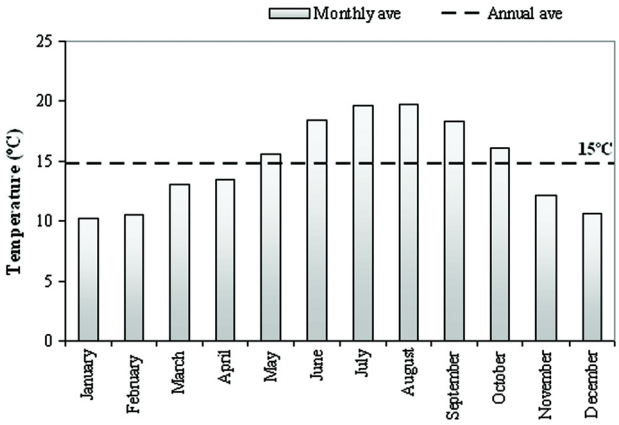

Figure 7 *Monthly and annual average of exterior temperature in Porto.*

presented higher condensation as a consequence of lower radiation.

Figure 6 also shows that there are very few accumulated degrees of condensation in every month, using any program, and this is due to the small differences between the dew point temperature and the surface temperature, which are, on average, around 0.2º C per hour. One the other hand, condensation occurs, on average, only half an hour per day during the year.

CONCLUSION

This brief review of heat, air, and moisture (HAM) analysis methods is the major outcome of this work. The review has shown that there are numerous hygrothermal models with a range of capabilities and that these models are important tools to better understand the real problems and to provide correct solutions.

The numerical results show that these programs are useful tools to simulate the undercooling phenomenon and assessing the exterior condensation on façades, providing that all relevant components of radiation exchange at the exterior surface are included in calculations. The models present similar results except when different inputs of long-wave radiation are used. In fact, it seems to be the key factor for the differences observed in the calculated values. Using cloud index information or measured long-wave radiation, even in the same model, provided the most significant differences.

Using accumulated degrees of condensation, a comparative measure of the risk of algae growth on exterior surfaces can be obtained. Since very small differences between surface and dew point temperature contribute to this indicator, the calculations are therefore demanding in terms of required precision.

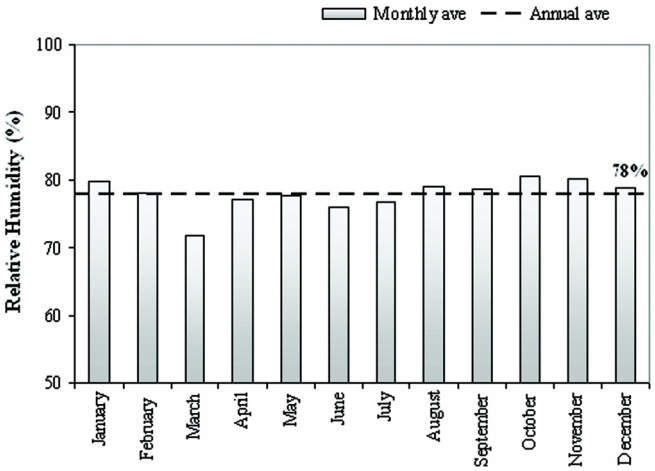

Figure 8 *Monthly and annual average of exterior relative humidity in Porto.*

In situ experiments are being performed to validate the numerical results and understanding which modelling strategy is the most adequate to simulate the undercooling phenomenon.

REFERENCES

Barreira, E., Freitas, V.P. and N. Ramos. 2009. Risk of ETICS defacement – A sensitivity analysis of the demand parameters. Proceedings of the 4th International Building Physics Conference, pp. 317-324, Istanbul, Turkey.

Djebbar, R., Kumaran, M.K., Van Reenen, D., and F. Tariku. 2002a. Hygrothermal modeling of building envelope retrofit measures in multiunit residential and commercial office buildings. Client Final Rep. No. B-1110.3, IRC/NRC, National Research Council, Ottawa, 187.

Djebbar, R., Kumaran, M.K., Van Reenen, D., and F. Tariku. 2002b. Use of hygrothermal numerical modeling to identify optimal retrofit options for high-rise buildings. Proceedings of the 12th International Heat Transfer Conference, Paper No. NRCC-45215, Grenoble, France, 1–6.

Canada Mortgage and Housing Corporation (CMHM). 2003. Review of hygrothermal models for building envelope retrofit analysis. Research highlights, Technical series 03-128.

Finkenstein, C. and P. Haupl. 2007. Atmospheric long wave radiation being a climatic boundary condition in hygrothermal building part simulation. 12th Symposium for Building Physics, vol. 2, pp. 617-624. Technische Universitat Dresden, Germany.

Galbraith, G.H., McLean, R.C. and J.S. Guo. 1997. The selection of appropriate flow potentials for moisture transport models. Fifth International Building Performance Simulation Association Conference, Prague, Czech Republic.

Hagentoft, C.E. 2001. Introduction to Building Physics. Studentlitteratur Ab.

Kalagasidis, A.S. 2004. HAM-Tools: An Integrated Simulation Tool for Heat, Air and Moisture Transfer Analyses in Building Physics. PhD Thesis, Chalmers University of Technology, Gothenburg, Sweden.

Karagiozis, A. 1993. Overview of the 2-D hygrothermal heat-moisture transport model LATENITE. Internal IRC/BPL Rep., National Research Council Canada, Ottawa.

Karagiozis, A., Salonvaara, M., and M.K. Kumaran. 1996. Numerical simulation of experimental freeze conditions in glass fibre insulation. Proceedings of the 4th Symposium on Building Physics in the Nordic Countries: Building Physics '96, VTT Building Technology, Finland, pp. 455–465.

Karagiozis, A. 1997. Analysis of the Hygrothermal Behaviour of Residential High-Rise Building Components. Client Report A-3052.4, IRC/NRC.

Kuenzel, H.M., and K. Kiessl. 1997. Calculation of Heat and Moisture Transfer in Exposed Building Components. International Journal of Heat Mass Transfer, 40 (1): 159–167.

Martin, M. and P. Berdahl. 1984. Summary of results from the spectral and angular sky radiation measurement program. Solar Energy, 33 (3-4): 241-252.

Meteotest. 2007. Meteonorm – Version 6.0. Meteotest, Bern, Switzerland.

Straube J., and E.F.P. Burnett. 2001. Overview of hygrothermal (HAM) analysis methods. In: Trechsel HR, editor.

ASTM manual 40-moisture analysis and condensation control in building envelopes, pp. 81–89.

Trechsel, H.R. 2001. Moisture Analysis and Condensation Control in Buildings. Manual 40. American Society for Testing and Materials (Chapter 6-Advanced Numerical Models for Hygrothermal Research by Karagiozis AN).